Synthesis and evaluation of microwave absorption properties of Fe_3O_4/Halloysite/polypyrrole nanocomposites

Sajjad Tabar Maleki[1], *Mohsen Babamoradi*[1] ✉, *Zoleikha Hajizadeh*[2], *Ali Maleki*[2], *Mojtaba Rouhi*[1]

[1]*Department of Physics, Iran University of Science and Technology, Tehran 16846–13114, Iran*
[2]*Catalysts and Organic Synthesis Research Laboratory, Department of Chemistry, Iran University of Science and Technology, Tehran 16846–13114, Iran*
✉ *E-mail: babamoradi@iust.ac.ir*

Published in Micro & Nano Letters; Received on 20th March 2020; Revised on 28th April 2020; Accepted on 13th May 2020

The Fe_3O_4 nanoparticles and Fe_3O_4/Halloysite nanotubes (HNTs) were synthesised by the co-precipitation method and Fe_3O_4/HNTs/polypyrrole (PPy) nanocomposites were synthesised by in situ polymerisation of pyrrole monomers on the surface of the Fe_3O_4/HNTs. The scanning electron microscopy images showed the uniform structure of nanocomposites. The Fourier transform infrared spectra revealed the characteristic peaks of Halloysite and PPy. The Fe_3O_4/HNTs/PPy nanocomposite exhibits a saturated magnetisation of 6.7 emu/g. The microwave absorption properties of Fe_3O_4/HNTs/PPy nanocomposites were investigated in the 8–12 GHz (X-band) range. The value of the minimum reflection loss was obtained − 26.2 dB at 11 GHz for the 3 mm thickness nanocomposite. The results showed the absorbing bandwidth below − 10 dB was broadened to 2.3 GHz.

1. Introduction: Electromagnetic pollution as a new kind of pollution in recent years has been introduced to our lives and has become a major concern due to the wide applications of electromagnetic waves. This kind of pollution has exceeded from effecting on industrial equipment to threatening life such as breaking down DNA strands, accelerating heart rates, brain tumours, and causing cancer [1, 2]. In this regard, the reduction of the adverse effects of electromagnetic waves is desirable as well as the technology of electromagnetic absorption in the microwave area. Microwave absorption is a valuable subject for commercial purposes, communications, military, civilian and many electronic and technological systems. For this reason, in recent years, the construction of a variety of absorbent coatings with suitable bandwidth has received a lot of attention [3, 4]. Various magnetic and dielectric materials have been extensively investigated as microwave absorbers to cover the interior and exterior surfaces [5–7].

In this regard, the use of nanoparticles in the fabrication of microwave absorbent coatings to achieve unique mechanical properties such as strength, high adhesion, small size, high level, and low mass density as much as possible with strong physical and chemical properties has attracted special attention [8, 9]. Therefore, nanocomposites are one of the most important achievements of using nanotechnology in the field of microwave protection. Among magnetic materials, Fe_3O_4 nanoparticles can be mentioned as desirable adsorbents [10, 11]. The use of only Fe_3O_4 nanoparticles cannot provide all demands of microwave absorption, so the integration of magnetic materials and conductive polymers into magnetic nanocomposites has been investigated. In other words, the ideal materials for microwave shielding are metals for their optimum conductivity and high dielectric and magnetic value, but they are restricted to be used widely because of their heavy weight, low flexibility, corrosion, and high cost [12–14]. The Fe_3O_4 nanoparticles absorb the waves by changing the molecular spins, and the conductive polymers, like resistors, which absorb the energy of the magnetic waves and convert it to heat in the absorption microwave process [15–17]. Therefore, coating the magnetic nanoparticles with a polymer is an effective way to enhance the stability of composites and extend their applications.

Polypyrrole (PPy), as an ordinary conductive polymer, has gained more attention due to its relatively easy preparation, excellent environmental stability and good electrical conductivity [18–20]. Halloysite can be used as a natural microporous nanotube to increase the ability of PPy for loading the metal nanoparticles [21]. In addition to its microporous property, it has high thermal and mechanical stability, green character, and low toxicity structure [22]. Halloysite for its low-cost property can be used as an alternative of carbon nanotubes (CNTs). Unlike CNTs, Halloysite nanotubes (HNTs) with rod geometry and non-intertwined properties, are easily dispersed in solutions or polymer matrices [23]. Synthesis of Fe_3O_4/PPy/CNT nanocomposites was reported by Yang *et al.* [24]. Their microwave absorption results showed that the addition of CNTs into Fe_3O_4/PPy composites enhances the minimum reflection loss (RL) from − 15.8 to − 25.9 dB. The core/shell nanocomposite, Fe_3O_4/PPy, was successfully synthesised by Li *et al.* [18]. The minimum reflectance loss was obtained by them as − 24.4 dB at 12.9 GHz with a thickness of 2.3 mm. The synthesis of FeOOH/polypyrrole (PPy)-α nanocomposite was reported by Xiao *et al.* [25]. They found the best [pyrrole]/[Fe^{2+}] ratio as 1.0 for obtaining the best microwave absorption property. The synthesis of polyaniline/$MnFe_2O_4$ nanocomposite was reported by Hosseini *et al.* [26]. They observed a minimum reflectance loss of −15.3 dB at a frequency of 10.4 GHz with a 1.4 mm thickness.

The co-precipitation method was used as a common method for synthesising Fe_3O_4 nanoparticles in the presence of a strong base. The pH is an important parameter and its value of about 11, procreates the magnetite (Fe_3O_4) phase. Therefore, ammonia and H_2O were used as a base for setting the pH according to (1) [27]

$$NH_3(aq) + H_2O(l) \rightarrow NH_4^+(aq) + OH^-(aq) \quad (1)$$

When the nanoparticles are prepared in the presence of oxygen, oxidation of Fe^{2+} to Fe^{3+} in the air is quite rapid and the procurement of the magnetite phase is difficult. To prevent this rapid oxidation, nitrogen gas (N_2) is usually used for synthesis. Synthesis in the presence of N_2 not only reduces the oxidation of the particles but also the size of the particles [28].

The purpose of this paper is to develop Fe_3O_4/HNTs/PPy nanocomposites to investigate the microwave absorption for the first time. Fe_3O_4/Halloysite syntheses as fillers and polypyrrole as a matrix have the possibility of investigating magnetic and electrical properties.

2. Experimental

2.1. Materials: $FeCl_3.6H_2O$, $FeCl_2.4H_2O$, and NH_3 were purchased from Merck. Halloysite nanotube and Pyrrole monomer were prepared from Sigma–Aldrich.

2.2. Synthesis of Fe_3O_4 nanoparticles: Fe_3O_4 nanoparticles were prepared by using a method as reported by Maleki *et al.* [29]. $FeCl_3{\cdot}6H_2O$ (1.165 g) and of $FeCl_2{\cdot}4H_2O$ (0.43 g) was added to 200 ml deionised water under nitrogen and stirred at 60°C. After 30 min, 20 ml solution of NH_4OH (NH_3, H_2O) was added drop by drop to the initial mixture for 2 h to pH value reached about 11. As the base was added, a black solution was formed. The stirring process of the solution was continued for about 2 h until the mixture was uniform. The final nanoparticles were dried for 24 h at room temperature.

2.3. Synthesis of Fe_3O_4/HNTs: Fe_3O_4/HNTs were prepared by following the procedure reported by Xie *et al.* with minor modifications [23]. At first, Halloysite (0.5 g), $FeCl_3{\cdot}6H_2O$ (1.165 g) and $FeCl_2{\cdot}4H_2O$ (0.43 g) were added to a 200 ml deionised water under the nitrogen gas at 60°C. After 30 min, 20 ml solution of NH_4OH (NH_3, H_2O) 8 mol/l was added drop by drop to the initial mixture. The final composites were dried for 24 h at room temperature.

2.4. Synthesis of Fe_3O_4/HNTs/PPy: To prepare Fe_3O_4/HNTs/PPy nanocomposite, the polymerisation was carried out in a 100 ml flask. Fe_3O_4/Halloysite (0.2 g) was mixed for 10 min in 40 ml of deionised water. Then 3 g of $FeCl_3.6H_2O$ was added to the solution. After 3 h, the pyrrole was added to this solution and stirred for 12 h at room temperature. The synthesised nanocomposite was washed with deionised water 3 times and then dried for 24 h at room temperature. Two different amounts of pyrrole were used in the synthesising Fe_3O_4/Halloysite/PPy (FHP) nanocomposites. FHP1 and FHP2 were synthesised with 0.3 and 0.4 ml of pyrrole, respectively. The schematic flowchart of the synthesis process of nanocomposites is demonstrated in Fig. 1.

3. Measurement: Scanning electron microscopy (SEM) images were taken with VEGA-TESCAN instrument. Vibrating-sample magnetometer (VSM) cure analysis was accomplished by LBKFB model, magnetic Kavir. Fourier transform infrared spectroscopy (FTIR) spectra of the composites were obtained on an FTIR-8400 Shimadzu Spectrum Scanner. Thermogravimetric analysis (TGA) was provided by Bahr-STA 504. The energy dispersive X-Ray (EDX) analysis was obtained by using a Numerix DXP-X10P instrument. Absorption properties were measured by a Vector Network Analysers (Agilent Technologies, E5071C) in the 8–12 GHz (X-band) range at room temperature. The nanocomposites (15 wt. %) were mixed uniformly with the paraffin at 60°C for obtaining the 3 mm thickness sample.

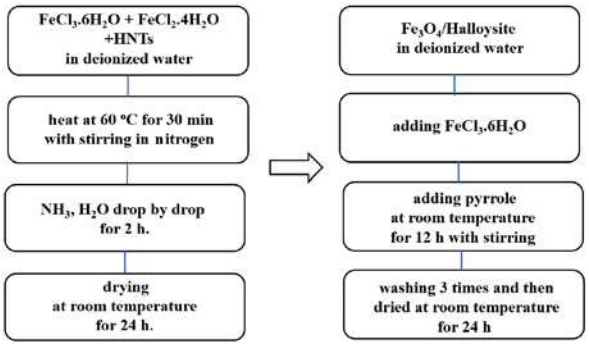

Fig. 1 *Schematic flowchart for the preparation of Fe_3O_4/HNTs/PPy nanocomposites*

4. Results and discussion

4.1. SEM: Fig. 2 shows the SEM images of the synthesised nanocomposites. The Fe_3O_4 nanoparticles and HNTs can be seen in Fig. 2*a*. The magnetic nanoparticles are agglomerated due to the attraction force among nanoparticles. The polymerisation of the pyrrole on the Fe_3O_4/HNTs is shown in Fig. 2*b*. The uniform structure can be seen in Fig. 2 in the result of pyrrole covering.

4.2. FTIR: Fig. 3 shows the FTIR spectra of the synthesised nanocomposites. In Fig. 3*a* the two near-peaks at 3692 and 3622 cm^{-1} are due to stretching vibrations of inner surface hydroxyl groups of HNTs [30]. The peaks near the 1000 cm^{-1} belong to the Si–O groups in the HNTs. The deformation of Si–O–Si, Al–O–Si, and O–H deformation of the inner hydroxyl groups of the peaks can be shown in the vicinity of 467, 536, and 910 cm^{-1}, respectively [31]. The broadband at 3430 cm^{-1} is due to the vibration traction of the hydroxyl groups of iron oxide [32]. The peak at 580 cm^{-1} is related to the vibration of the Fe–O band. The peaks near 1308, 1034 and 907 cm^{-1} confirm the chemical composition of PPy [24]. The peaks at around 1543 and 1466 cm^{-1} show pyrrole ring and conjugated C–N stretching, respectively. The peaks at about 1045 and 927 cm^{-1} show the out-of-plane vibrations of C–H and ring deformation. Figs. 3*b* and *c* represent that the Fe_3O_4/PPy and Fe_3O_4/HNTs/PPy composites have the characteristic peaks of both the Fe_3O_4 and PPy entities. These results indicate the presence of PPy polymers in composite materials.

4.3. EDX: The result of the EDX analysis of the Fe_3O_4/HNTs/PPy nanocomposites is shown in Fig. 4. This confirms the presence of carbon, oxygen, silicon, aluminium, nitrogen and iron elements in the nanocomposite appropriately. No other impurity elements

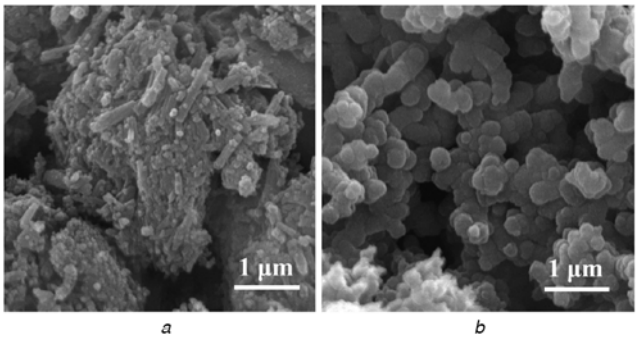

Fig. 2 *SEM images of*
a Fe_3O_4/Halloysite
b FHP nanocomposites

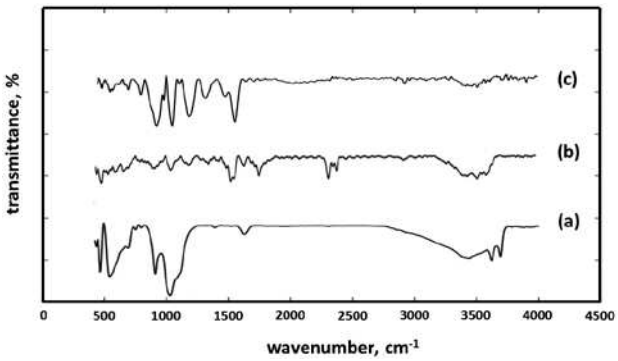

Fig. 3 *FTIR spectrum of*
a Fe_3O_4/HNTs
b Fe_3O_4/PPy
c Fe_3O_4/HNTs/PPy nanocomposites

doi: 10.1049/mnl.2020.0165

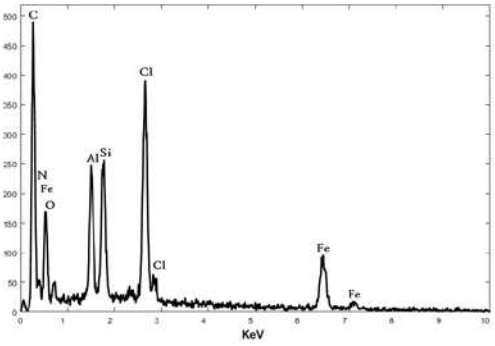

Fig. 4 *EDX analysis of the Fe_3O_4/HNTs/PPy nanocomposite*

were observed in the spectra, implying that the synthesised nanocomposite has good quality.

4.4. Magnetic properties: The magnetisation versus applied magnetic field of the nanocomposites is shown in Fig. 5. The thinner magnetic curve of the sample produced in the VSM analysis means a soft magnetic material, which is magnetised easily by applying a magnetic field. The Fe_3O_4/HNTs/PPy nanocomposite exhibits a saturated magnetisation of 6.7 emu/g. Compared to Fe_3O_4 nanoparticles (65.4 emu/g) [24], the reduction of saturated magnets for Fe_3O_4/HNTs/PPy nanocomposites is due to the presence of non-magnetic materials on the surface of the nanoparticles. The PPy and HNTs reduce the saturation magnetism significantly [18, 29].

4.5. TGA: The results of the TGA of the nanocomposite are illustrated in Fig. 6. The weight loss of about 4% at temperature 110°C is attributed to the expulsion of moisture in the polymer [33, 34]. The degradation of PPy is started at a temperature

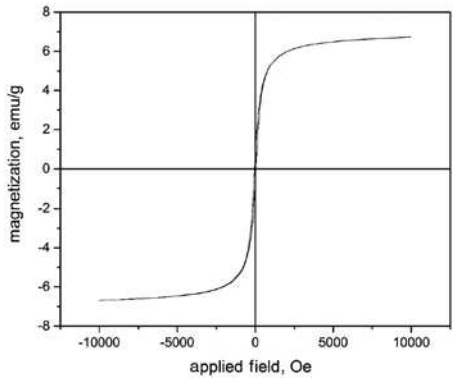

Fig. 5 *Magnetic hysteresis loops of Fe_3O_4/HNTs/PPy nanocomposite at room temperature*

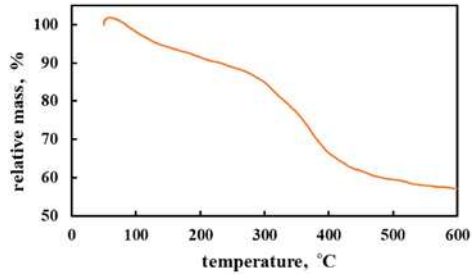

Fig. 6 *TGA curves of the Fe_3O_4/HNTs/PPy nanocomposite*

higher than 220°C and a weight loss of 12% at 250°C. Temperature above 250°C causes the decomposition of PPy and results in a weight loss of about 52% up to 600°C. This weight loss can be attributed to the release of C, H and N moieties of PPy unit. A sharp loss in mass at 300°C, is due to the thermal degradation of the PPy chains [35]. The Fe_3O_4 nanoparticles are stable up to 600°C and the weight loss can be attributed to the PPy and Halloysite.

4.6. Microwave absorption properties: The microwave absorption properties of the composites are related to their complex permittivity $\varepsilon = \varepsilon' + j\varepsilon''$ and permeability $\mu = \mu' + j\mu''$. As it is obvious, the real parts of complex permittivity and permeability show the storage of electric and magnetic energy, respectively. While the imaginary parts of the complex permittivity and permeability show the loss of electrical and magnetic energy of the sample. Fig. 7 shows the real and imaginary parts of the permeability and permittivity of Fe_3O_4/HNTs/PPy composite as a function of frequency. The ε' value is about 8–10 and ε'' is about 4–5.5. It can be seen that the real part (ε') and imaginary part ε'' of complex permittivity decrease as the frequency increases. The ε' of raw Fe_3O_4 is calculated as 8.5 by Cheng *et al*. [36]. For obtaining the good performance of absorption, the value of real permittivity should be in moderate value (10–20) [37] and the ε' of the synthesised sample is in this range. On the other hand, the value of ε'' for raw Fe_3O_4 is measured as about 0.5 while its larger value is good for the absorption process [36]. The imaginary permittivity of the nanocomposite is higher than other microwave absorption materials [38, 39]. The better imaginary part implies a greater loss of dielectric and causes more electromagnetic energy which can be converted into heat energy. This phenomenon may be due to dielectric loss at high frequencies caused by PPy shell. The core/shell microstructure creates an additional interface and interfacial polarisation at the nanoparticle surface. In other words, the enhancing particle polarisation increases the permittivity values of nanocomposites and this relates to the particle surface conductivity of PPy [24]. Therefore, it can be deduced that the higher imaginary part can improve the microwave absorption property of the sample [18].

Since larger values of ε'' and μ'' usually lead to better adsorption performance, but do not guarantee the best possible performance and must be considered with other parameters such as ε', μ', matching frequency and matching thickness [24]. The microwave absorbing attributes of the materials can be determined by reflection loss (RL). The RL of the absorber composites is supported by a perfect conductor and can be computed with the complex permittivity and permeability for the given frequency and absorber thicknesses. The RL of the composites can be computed by exerting

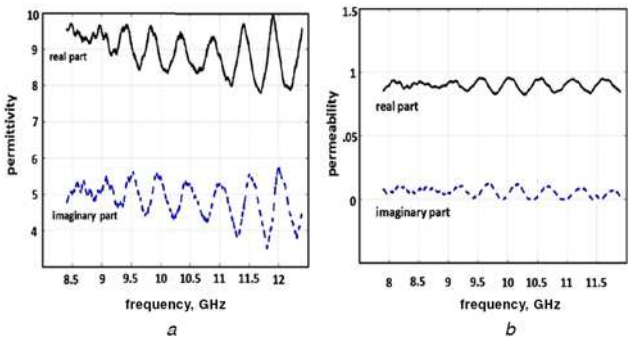

Fig. 7 *The change in dielectric real (black color line: ε') and imaginary part (blue color line: ε")*
a magnetic real part (black color line: μ′) and imaginary part (blue color line: μ″)
b of the Fe_3O_4/HNTs/PPy nanocomposites

the following equation and the measured electromagnetic parameters [40]:

$$Z_{\text{in}} = \sqrt{\frac{\mu_{\text{r}}}{s_{\text{r}}}} \tanh\left(\text{j}\frac{2\pi fd}{c}\sqrt{\mu_{\text{r}}\varepsilon_{\text{r}}}\right) \quad (2)$$

$$\text{RL} = 20\log\left|\frac{Z_{\text{in}}-1}{Z_{\text{in}}+1}\right| \quad (3)$$

where RL shows the reflection loss in decibel unit, Z_{in} is the normalised input impedance relating to the impedance in free space, f is the microwave frequency, d is the thickness of the absorbing layer, c is the velocity of the electromagnetic wave in vacuum, and ε_{r} and μ_{r} are the complex relative permittivity and permeability, respectively. The equation for impedance matching ($Z_{\text{in}} = 1$) becomes:

$$1 = \sqrt{\frac{\mu_{\text{r}}}{\varepsilon_{\text{r}}}} \tanh\left(\text{j}\frac{2\pi fd}{c}\sqrt{\mu_{\text{r}}\varepsilon_{\text{r}}}\right) \quad (4)$$

The matching frequency (f_{m}) and thickness (d_{m}) can be specified by using (4). The physical mechanism of the impedance matching of the absorber can be defined as two interactions, i.e. the scattering related to the mediocre impedance and the dissipation related to the imaginary parts of the complex-valued permittivity and permeability. For a composite absorber with equal thickness, it is specific that the matching frequency (f_{m}) changes to lower frequencies by increasing the weight percent of absorbent fillers. Also, the f_{m} changes to the lower frequencies by increasing the thickness of the absorbers [41]. Based on the equations above, a typical relationship between RL and frequency for the samples (the weight of composite in the paraffin is 15 wt%) in the 8–12 GHz range and layer thickness of 3 mm is shown in Fig. 8. It is clearly viewed that the samples have suitable microwave absorption properties. The lowest RL of −10.68 dB is found at 11.4 GHz for Fe_3O_4/PPy. Compared to Fe_3O_4 (about −4 dB) [24] with the addition of polypyrrole, the RL rate has increased significantly. The presence of PPy reduces the effect of the magnetic connection between the nanoparticles, increasing the anisotropy of the effective surface of the nanoparticles, which contributes to better coordination between the dielectric loss and the magnetic loss [18]. Reduction of the magnetic-coupling between nanoparticles and increase of the effective surface anisotropy of nanoparticles can be obtained by the presence of PPy. The dielectric loss ability of PPy and its role for match the dielectric loss and magnetic loss will result in the excellent microwave absorption properties of PPy composites.

A better microwave absorption efficiency in the FHP samples was obtained. The relating minimum RL of −24.6 and −26.2 dB is achieved at about 11 GHz for FHP1 and FHP2 nanocomposites, respectively. By comparing the RL of the FHPs with the Fe_3O_4/PPy, it is observed that by adding HNTs to the Fe_3O_4/PPy, the amount of RL increases and moves to low frequencies. The absorbing broadband (exceeding −10 dB) of FHP composite is 2.3 GHz which is much broader than the Fe_3O_4/PPy sample. As it is shown in Fig. 8, by increasing the PPy amount in FHP composites, the RL value increases. The reduction in FHP1 and FHP2 reflection loss can be explained to larger dielectric loss and magnetic loss than other samples. To shifting the RL minimum and absorbing broadband to lower frequencies, one can increase the weight percent of absorbent fillers to procure better amounts of ε', ε'', μ', and μ'' or increase the thickness of the absorbers. For all composites, the values of ε' and ε'' depend on the amount of PPy and HNTs, and this method can be used to adjust the adsorbent by loss of optimum reflectance in the target frequency band. Yang *et al.* [24] calculated the minimum RL of Fe_3O_4/polypyrrole/carbon nanotube composites as −25.9 dB. Our results are comparable with their results and also suggest a cheaper and more biocompatible alternative for CNTs. The Fe_3O_4-coated CNTs reveals the good microwave absorption properties in comparison with Fe_3O_4. This increase in microwave absorption properties can be related to these features [42]: (i) Low reflection on the surface, which comes from impedance matching between the wave absorbers and free space of CNTs. (ii) Multiple reflection from small nanoparticles which transmit the incident waves into the composites. (iii) Space charge accumulation at the interface of Fe_3O_4-coated CNTs. (iv) Collective interfacial dipoles from closed-spaced nanoparticles which is beneficial for dielectric loss by amplifying the response to incident microwave. These aspects of CNTs in combination with Fe_3O_4 can be provided by Halloysite as a natural microporous nanotube. In addition high surface area with more active sites is desirable for dissipating and scattering microwaves which can be reached by CNTs or HNTs as their alternatives.

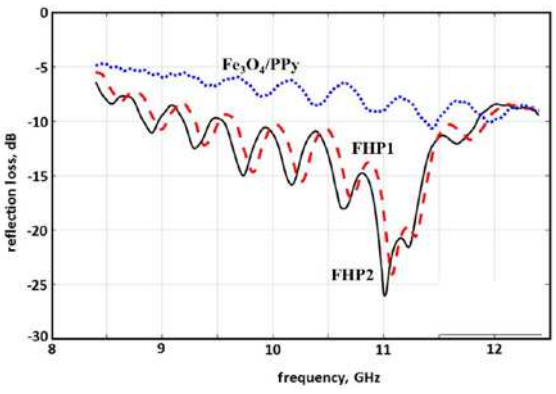

Fig. 8 *RL of Fe_3O_4/PPy and Fe_3O_4/HNTs/PPy (FHP1 and FHP2) nanocomposites*

5. Conclusion: The FHP composites were synthesised by polymerising the conductive monomer (pyrrole) on the surface of Fe_3O_4/Halloysite. The magnetic investigation revealed that the Fe_3O_4/PPy nanocomposite is ferromagnetic at room temperature and its saturation magnetisation (M_S) is 6.7 emu/g. The results show that by adjusting the amount of dielectric polymer, PPy, the RL can be obtained as −26.2 dB. The results show that the HNTs as a cheaper alternative for CNTs, enhance the absorption of Fe_3O_4/PPy due to their high surface-to-volume ratio. The enhancing of the RL value by adding the Halloysite can be related to its microporous structure.

6. Acknowledgments: The authors gratefully acknowledge the partial support from the Research Council of the Iran University of Science and Technology.

7 References

[1] Kasevich R.S.: 'Cellphones, radars, and health'. *IEEE Spectr.*, 2002, **39**, (8), pp. 15–16
[2] Baan R., Grosse Y., Lauby-Secretan B., *ET AL.*: 'Carcinogenicity of radiofrequency electromagnetic fields', *Lancet Oncol.*, 2011, **12**, (7), pp. 624–626
[3] Roh J.S., Chi Y.S., Kang T.J., *ET AL.*: 'Electromagnetic shielding effectiveness of multifunctional metal composite fabrics', *Tex. Res. J.*, 2008, **78**, (9), pp. 825–835
[4] Shahzad F., Alhabeb M., B. Hatter C., *ET AL.*: 'Electromagnetic interference shielding with 2D transition metal carbides (MXenes)', *Science*, 2016, **353**, (6304), pp. 1137–1140
[5] Tong G., Hong M., Guan J., *ET AL.*: 'Enhanced microwave absorption properties of Fe nanotubes fabricated by a facile gas bubble-engaged assembly technique', *Micro Nano Lett.*, 2011, **6**, (8), pp. 722–724
[6] Haddad A., Ouldbrahim I, Azzaz M.: 'Structure, magnetic and microwave studies of mechanically alloyed powders $Fe_{45}Ni_{35}Co_{20}$', *Micro Nano Lett.*, 2018, **13**, pp. 974–978
[7] Salimbeygi G., Nasouri K., Shoushtari A.M., *ET AL.*: 'Fabrication of polyvinyl alcohol/multi-walled carbon nanotubes composite

doi: 10.1049/mnl.2020.0165

electrospun nanofibres and their application as microwave absorbing material', *Micro Nano Lett.*, 2013, **8**, (8), pp. 455–459
[8] Oikonomou A., Giannakopoulou T., Litsardakis G.: 'Design, fabrication and characterization of hexagonal ferrite multi-layer microwave absorber', *J. Magn. Magn. Mater.*, 2007, **316**, (2), pp. e827–e830
[9] Pawar S., Biswas. S., Kar G.P., *ET AL.*: 'High frequency millimetre wave absorbers derived from polymeric nanocomposites', *Polymer*, 2016, **84**, pp. 398–419
[10] Wei S., Yan R., Shi B., *ET AL.*: 'Characterization of flexible radar-absorbing materials based on ferromagnetic nickel micron-fibers', *J. Ind. Text*, 2018, **49**, (1), pp. 58–70
[11] Nam Y.W., Choi J.H., Huh J.M., *ET AL.*: 'Thin broadband microwave absorber with conductive and magnetic materials coated on a glass fabric', *J. Compos. Mater.*, 2018, **52**, (10), pp. 1413–1420
[12] Yang Y., Gupta M.C., Dudley K.L., *ET AL.*: 'Novel carbon nanotube – polystyrene foam composites for electromagnetic interference shielding', *Nano Lett.*, 2005, **5**, (11), pp. 2131–2134
[13] Li N., Huang Y., Du F., *ET AL.*: 'Electromagnetic interference (EMI) shielding of single-walled carbon nanotube epoxy composites', *Nano Lett.*, 2006, **6**, (6), pp. 1141–1145
[14] Sambyal P., Dhawan S.K., Preeti G., *ET AL.*: 'Synergistic effect of polypyrrole/BST/RGO/Fe_3O_4 composite for enhanced microwave absorption and EMI shielding in X-band', *Cur. Appl. Phys.*, 2018, **18**, (5), pp. 611–618
[15] Lederer P.: 'An introduction to radar absorbent materials (RAM)', 1986, Royal Signals and Radar Establishment Malvern (England)
[16] Teber A., Unver I., Kavas H., *ET AL.*: 'Knitted radar absorbing materials (RAM) based on nickel–cobalt magnetic materials', *J. Magn. Magn. Mater.*, 2016, **406**, pp. 228–232
[17] Singh D., Kumar A., Meena S., *ET AL.*: 'Analysis of frequency selective surfaces for radar absorbing materials', *Prog. Electromagn. Res. B.*, 2012, **38**, pp. 297–314
[18] Li Y., Chen G., Li Q., *ET AL.*: 'Facile synthesis, magnetic and microwave absorption properties of Fe_3O_4/polypyrrole core/shell nanocomposite', *J. Alloys Compd.*, 2011, **509**, (10), pp. 4104–4107
[19] Wang L.-X., Li X.-G., Yang Y.-L: 'Preparation, properties and applications of polypyrroles', *React. Funct. Polym.*, 2001, **47**, (2), pp. 125–139
[20] Ramya R., Sivasubramanian R., Sangaranarayanan M.: 'Conducting polymers-based electrochemical supercapacitors – progress and prospects', *Electrochim. Acta*, 2013, **101**, pp. 109–129
[21] Li L., Wang F., Lv Y., *ET AL.*: 'Halloysite nanotubes and Fe_3O_4 nanoparticles enhanced adsorption removal of heavy metal using electrospun membranes', *Appl. Clay Sci.*, 2018, **161**, pp. 225–234
[22] Papoulis D.: 'Halloysite based nanocomposites and photocatalysis: a review', *Appl. Clay Sci.*, 2019, **168**, pp. 164–174
[23] Xie Y., Chang P.R., Wang S., *ET AL.*: 'Preparation and properties of halloysite nanotubes/plasticized Dioscorea opposita Thunb. starch composites', *Carbohydr. Polym.*, 2011, **83**, (1), pp. 186–191
[24] Yang R.-B., Reddy P.M., Chang C.J., *ET AL.*: 'Synthesis and characterization of Fe_3O_4/polypyrrole/carbon nanotube composites with tunable microwave absorption properties: role of carbon nanotube and polypyrrole content', *Chem. Eng. J.*, 2016, **285**, pp. 497–507
[25] Xiao H.-M., Zhang W.-D., Fu S.-Y.: 'One-step synthesis, electromagnetic and microwave absorbing properties of α-FeOOH/polypyrrole nanocomposites', *Compos. Sci. Technol.*, 2010, **70**, (6), pp. 909–915
[26] Hosseini S.H., Mohseni S.H., Asadnia A., *ET AL.*: 'Synthesis and microwave absorbing properties of polyaniline/$MnFe_2O_4$ nanocomposite', *J. Alloys Compd.*, 2011, **509**, (14), pp. 4682–4687
[27] Faiyas A.P.A., Vinod E.M., Joseph J., *ET AL.*: 'Dependence of pH and surfactant effect in the synthesis of magnetite (Fe_3O_4) nanoparticles and its properties', *J. Magn. Magn. Mater.*, 2010, **322**, pp. 400–404
[28] Maity D., Agrawal D.C.: 'Synthesis of iron oxide nanoparticles under oxidizing environment and their stabilization in aqueous and non-aqueous media', *J. Magn. Magn. Mater.*, 2007, **308**, pp. 46–55
[29] Maleki A., Hajizadeh Z., Firouzi-Haji R.: 'Eco-friendly functionalization of magnetic halloysite nanotube with SO_3H for synthesis of dihydropyrimidinones', *Microporous Mesoporous Mater.*, 2018, **259**, pp. 46–53
[30] Luo P., Zhao Y., Zhang B., *ET AL.*: 'Study on the adsorption of neutral red from aqueous solution onto halloysite nanotubes', *Water Res.*, 2010, **44**, (5), pp. 1489–1497
[31] Tierrablanca E., García J.R., Roman P., *ET AL.*: 'Biomimetic polymerization of aniline using hematin supported on halloysite nanotubes', *Appl. Catal., A*, 2010, **381**, (1–2), pp. 267–273
[32] Hsieh S., Huang B.Y., Hsieh S.L., *ET AL.*: 'Green fabrication of agar-conjugated Fe_3O_4 magnetic nanoparticles', *Nanotechnology*, 2010, **21**, (44), p. 445601
[33] Mavinakuli P., Wei S., Wang Q., *ET AL.*: 'Polypyrrole/silicon carbide nanocomposites with tunable electrical conductivity', *J. Phys. Chem. C*, 2010, **114**, (9), pp. 3874–3882
[34] Guo Z., Shin K., Karki A.B., *ET AL.*: 'Fabrication and characterization of iron oxide nanoparticles filled polypyrrole nanocomposites', *J. Nanopart. Res.*, 2009, **11**, (6), pp. 1441–1452
[35] Jang J., Yoon H.: 'Novel fabrication of size-tunable silica nanotubes using a reverse-microemulsion-mediated Sol–gel method', *Adv. Mater.*, 2004, **16**, (9–10), pp. 799–802
[36] Cheng Y., Li Y., Ji G., *ET AL.*: 'Magnetic and electromagnetic properties of Fe_3O_4/Fe composites prepared by a simple one-step ball-milling', *J. Alloys Compd.*, 2017, **708**, pp. 587–593
[37] Wang J., Wang J., Zhang B., *ET AL.*: 'Combined use of lightweight magnetic Fe_3O_4-coated hollow glass spheres and electrically conductive reduced graphene oxide in an epoxy matrix for microwave absorption', *J. Magn. Magn. Mater.*, 2016, **401**, pp. 209–216
[38] Dong X.L., Zhang X.F., Huang H., *ET AL.*: 'Enhanced microwave absorption in Ni/polyaniline nanocomposites by dual dielectric relaxations', *Appl. Phys. Lett.*, 2008, **92**, (1), p. 013127
[39] Xianguo L., Dianyu G., Panju S.H., *ET AL.*: 'Fluorescence and microwave-absorption properties of multi-functional ZnO-coated α-Fe solid-solution nanocapsules', *J. Phys. D: Appl. Phys.*, 2008, **41**, (17), p. 175006
[40] Zuo W.L., Qiao L., Chi X., *ET AL.*: 'Complex permeability and microwave absorption properties of planar anisotropy $Ce_2Fe_{17}N_3-\delta$ particles', *J. Alloys Compd.*, 2011, **509**, (22), pp. 6359–6363
[41] Kim S., Babbar V.K., Razdan A., *ET AL.*: 'Complex permeability and permittivity and microwave absorption of ferrite-rubber composite at X-band frequencies', *IEEE Trans. Magn.*, 1991, **27**, (6), pp. 5462–5464
[42] Li N., Gui-Wen Huang G.W., Li Y.Q., *ET AL.*: 'Enhanced microwave absorption performance of coated carbon nanotubes by optimizing the Fe_3O_4 nanocoating structure', *ACS Appl. Mater. Interf.*, 2017, **9**, pp. 2973–2983